J. Phys. Chem. A **1997,** *101,* 4375−4383 **4375**

Thermal Decomposition Pathways of 1,3,3-Trinitroazetidine (TNAZ), Related 3,3-Dinitroazetidium Salts, and ^{15}N, ^{13}C, and ^{2}H Isotopomers

Jimmie Oxley,* James Smith, Weiyi Zheng, Evan Rogers, and Michael Coburn

Department of Chemistry, University of Rhode Island, Kingston, Rhode Island 02881-0809

Received: January 7, 1997; In Final Form: April 15, 1997⊗

The thermal decomposition of 1,3,3-trinitroazetidine (TNAZ) and related 3,3-dinitroazetidium (DNAZ$^+$) salts was examined neat and in solution. TNAZ kinetics were found (160−250 °C) to be first-order and nearly identical neat and in benzene, with an activation energy of 46.6 kcal/mol (195 kJ/mol). The DNAZ$^+$ salts were less thermally stable than TNAZ, and neat did not decompose in a first-order fashion. However, in aqueous solution the DNAZ$^+$ salts did decompose following first-order kinetics; their rates were similar with minor differences apparently related to the strength of the anion as a conjugate base. Like simple nitramines such as dimethylnitramine, TNAZ tended to form N_2O rather than N_2, but unlike other nitramines it formed about as much NO as N_2O. TNAZ isotopomers labeled with ^{13}C and with ^{15}N were prepared and used to identify the origin of the decomposition gases and the identity of the condensed-phase products. Early in the decomposition of TNAZ, most of the NO came from the nitro group attached to the azetidium ring nitrogen. Most of the N_2O was the result of the nitro groups interacting with each other, while the majority of the N_2 contained one nitrogen from the ring. Many condensed products have been identified, but five stand out because they are formed in the thermolysis of TNAZ and the three DNAZ$^+$ salts [NO_3^-, Cl^-, $N(NO_2)_2^-$]. These are 3,5-dinitropyridine (**M**, always a minor product), 1-formyl-3,3-dinitroazetidine (**L**), 1,3-dinitroazetidine (**K**), 1-nitroso-3,3-dinitroazetidine (**E**), and 1-nitroso-3-nitroazetidine (**G**); the identity of the first four has been confirmed by use of authentic samples. Of these five, the last four have been shown to interconvert with TNAZ and each other under the conditions of these experiments. This study confirms the presence of two competitive TNAZ decomposition pathways. Under the conditions of this study, N−NO$_2$ homolysis is slightly favored, but products, such as **K**, resulting from C−NO$_2$ scission, are also well represented.

Introduction

We have previously reported the decomposition kinetics of a number of pure nitramines, both simple nitramines, such as dimethylnitramine (DMN) and diisopropylnitramine (DIPN),[1] and multifunctional nitramines such as 1,3,5-trinitro-1,3,5-triazocyclohexane (RDX) and 1,3,5,7-tetranitro-1,3,5,7-tetrazocine (HMX).[2] For these compounds we found first-order kinetics and nitrosoamine products formed by at least one decomposition pathway. Now we examine a new[3] multifunctional energetic material, 1,3,3-trinitroazetidine (TNAZ), which has both N−NO$_2$ and C−NO$_2$ linkages. It is unique among the energetic nitramines in that it can be held above its melting temperature (101 °C)[4] without immediate decomposition. This property makes it probable that like 2,4,6-trinitrotoluene (TNT), TNAZ will be processed in the liquid phase; therefore, a thorough study of its thermal stability is required. One question of interest to us was which X−NO$_2$ linkage would be weakest. Politzer predicted an energy difference in products 1 and 2 of only 2 kcal (Figure 1).[5] Although the melt-phase mixtures of TNAZ have recently been reported,[6] the few reports of its thermal decomposition are limited to examination of its decomposition gases.[7,8] The methodology of our study was to determine the kinetics of TNAZ decomposition and compare them to pure nitramines and to identify TNAZ decomposition products. To aid in the latter study, salts related to TNAZ, the salts of 3,3-dinitroazetidine (DNAZ), were examined in terms of their decomposition kinetics and products.

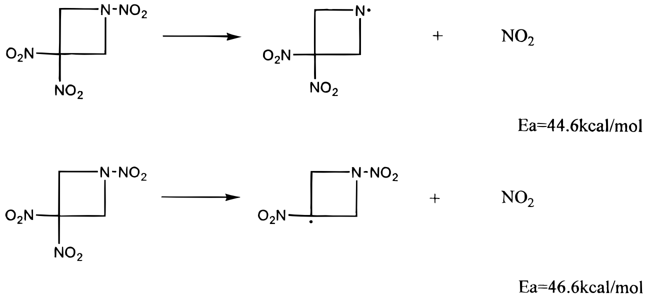

Figure 1. Theoretical bond dissociation energies for TNAZ (ref 5).

Experimental Section

TNAZ was provided by Eglin Air Force Base. 3,3-Dinitroazetidium salts were synthesized by Dr. Michael Hiskey of Los Alamos National Laboratory; 1,3-dinitroazetidine and 1-formyl-3,3-dinitroazetidine were provided by Drs. Alan Marchand, University of North Texas, and Paritosh Dave, Geo-Centers, NJ. Synthesis of TNAZ isotopomers is described elsewhere.[9] In sealed glass tubes (2.4 mm i.d. × 60−70 mm long, volume about 200 μL),[1] thermolyses were performed isothermally in the temperature range 160−280 °C for TNAZ and 100−200 °C for dinitroazetidium salts. For neat thermolyses 0.2−0.3 mg of TNAZ or 0.4−0.5 mg of dinitroazetidium salts was used; for solution thermolyses about 50 μL of 1% TNAZ solution in acetone, benzene, or methanol or 1% dinitroazetidium (DNAZ$^+$) salts in aqueous solution were used. After thermolysis, the fraction remaining was assessed by dissolving samples in acetone or methanol and analyzing by liquid chromatography. For most samples, first-order rate constants were determined using at least six data points out to 70% decomposition. The thermolyses of the neat dinitroazetidium salts were the exception; first-order rate constants were derived from only the first 30% of the decompositions. Arrhenius parameters were determined using rate constants for at least four temperatures.

A Hewlett Packard (HP) high-performance liquid chromatograph (HPLC) Model 1084 B equipped with a 20 μL sample

---

⊗ Abstract published in *Advance ACS Abstracts,* June 1, 1997.

TABLE 1: TNAZ Rate Constants, Neat, in Solution (1%), and with Additives

sample	no. data	temp range (°C)	E_a (kcal/mol)	A (s^{-1})	R^2	solvent[a]/additive	rate const at 240 °C	DKIE
TNAZ	7	160−250	46.6	3.55E+17[b]	0.99	neat	4.84E−03	
TNAZd4						neat	3.69E−03	1.31
TNAZ	6	160−260	40.3	5.61E+14	1.00	benzene	5.32E−03	
TNAZ						benzene-d_6	5.03E−03	1.06
TNAZd4						benzene	3.86E−03	1.38
TNAZ	7	189−280	43.6	2.89E+16	0.99	acetone	8.47E−03	
TNAZ						acetone-d_6	2.28E−03	3.71
TNAZ	4	180−240	30.7	2.62E+11	0.96	methanol	2.05E−02	
TNAZ						MeOH-d_4	1.06E−02	1.93
TNAZ						+10% DPA	5.40E−03	
TNAZ						+5% HNO_3	5.26E−03	
TNAZ						+50% H_2O	4.74E−03	
TNAZ						H_2O	1.52E−02	
TNAZ						+50% RDX	2.74E−04[c]	
TNAZ						neat	1.36E−04[c]	
NODNAZ						acetone	1.57E−03	

[a] 1% wt TNAZ in solvents. [b] Read as 3.55 × 10^{17}. [c] At 200 °C.

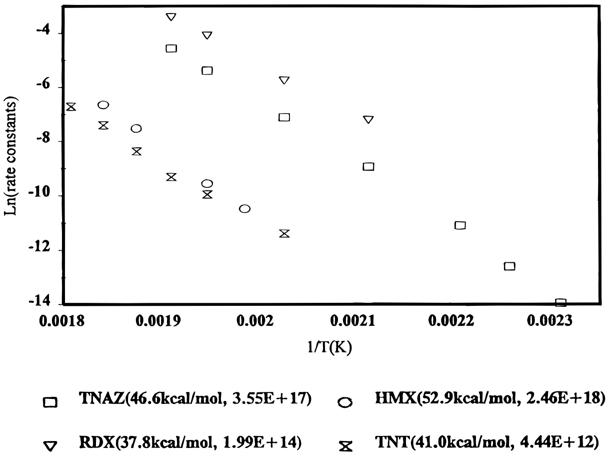

Figure 2. Arrhenius kinetic plots of TNAZ and other energetic materials.

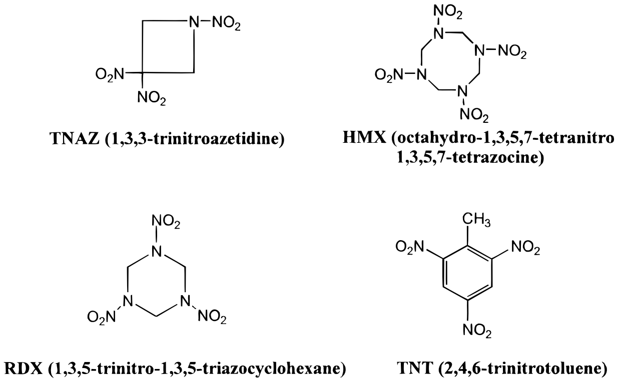

TNAZ (1,3,3-trinitroazetidine)

HMX (octahydro-1,3,5,7-tetranitro 1,3,5,7-tetrazocine)

RDX (1,3,5-trinitro-1,3,5-triazocyclohexane)

TNT (2,4,6-trinitrotoluene)

Figure 3. Energetic materials used as explosives.

loop and a Waters 486 tunable absorbance detector was employed to determine the rate constants. An Alltech Econosphere C-18, 5 μm (250 mm × 4.6 mm), reversed phase column and an eluent of $CH_3OH/THF/H_2O$(32:4.8:63.2) was used to separate TNAZ and its products. A Dionex AS-11 anion column and a mobile phase of 2 mM NaOH/40% CH_3CN (flow 1.0 mL/min) and a UV detector (214 nm) were used to analyze the DN^-, NO_3^-, and NO_2^- anions. The concentration of Cl^- did not vary much during the course of the thermolysis; it was determined using a Dionex Model 2000i/sp ion chromatograph equipped with a AS-4A column and conductivity detector and using a mobile phase of 2.2 mM Na_2CO_3/0.7 mM $NaHCO_3$. The cations $DNAZ^+$ and NH_4^+ were separated and detected using a Waters IC-Pak cation M/D column with a mobile phase of 0.1 mM EDTA/3 mM HNO_3 (flow, 1.0 mL/min) and a Waters 431 conductivity detector.

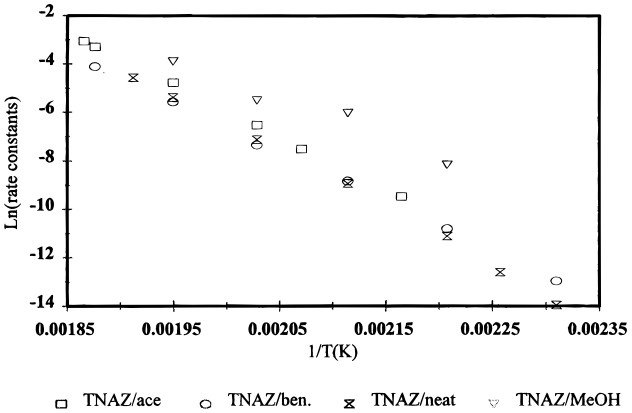

Figure 4. Arrhenius plots of TNAZ neat and 1% TNAZ in various solvents.

The separation, identification, and quantification of gaseous products was accomplished using a HP 5890 gas chromatograph equipped with a Alltech Heyesep DB 100/120 (30 ft × 1/8 in.) packed column and a thermal conductivity detector (GC-TCD). The oven temperature was held at 35 °C for 6 min and then ramped at 15 °C/min to 180 °C. Certified standard gases (Scott Speciality Gas Co.) were used to generate standard curves. Identification of gases was by retention times and by comparison to the standard gases. Quantification was achieved using standard curves of area versus concentration of the standard gases. A HP 5890 gas chromatograph equipped with an electronic pressure control system, a poraPLOT Q (Chrompack) capillary column (25 m × 0.25 mm i.d.), and a HP 5971 electron impact quadrupole mass spectrometer was used for analysis of gases produced from the decomposition of labeled TNAZ.[10] The capillary tubes containing samples were evacuated and sealed. After thermolysis sample tubes were broken in a flexible Teflon tube connected in line with the GC carrier gas and just before the injector and electronic pressure control system. The decomposition gases flow into the injector (split ratio 15:1) and onto the column. The oven temperature was held at −80 °C for 5 min and then ramped at 15 °C/min to 150 °C.

Differential scanning calorimetry (DSC) and thermal gravimetric analysis (TGA) were used to determine the relative thermal stability of TNAZ and dinitroazetidium salts. DSC measurements used a Perkin-Elmer (PE) DSC-4 or a TA Instruments modulated DSC-2910, under N_2 flow using an indium calibration standard. DSC samples were weighed (0.2−0.5 mg) and sealed into glass capillary tubes (0.058−0.059 in. o.d. and 0.011−0.012 in. wall). These were placed in aluminum cradles in the DSC head and heated over the range 40−450 °C at a scan rate of 20 °C/min. TGA experiments used a TGA-2

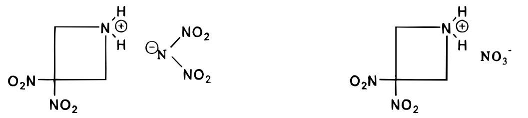

DNAZDN(3,3-dinitroazetidinium dinitramidate) **DNAZNO$_3$**(3,3-dinitroazetidinium nitrate)

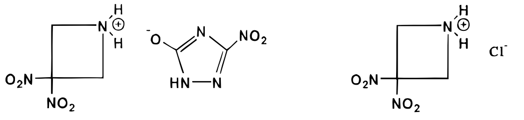

DNAZNTO(3,3-dinitroazetidinium 5-nitro-1,2,4-triazol-3-onate) **DNAZCl** (3,3-dinitroazetidinium chloride)

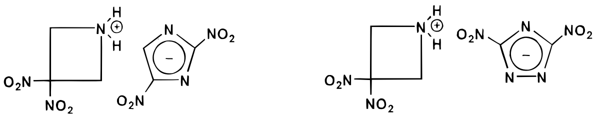

DNAZDNI(3,3-dinitroazetidinium 2,4-dinitroimidazolate) **DNAZDNT**(3,3-dinitroazetidinium 3,5-dinitro-1,2,4-triazolate)

Figure 5. 3,3-Dinitroazetidium (DNAZ$^+$) salts examined by thermal analysis.

TABLE 2: DSC and TGA of DNAZ Salts and TNAZ

DSC (Scan Rate: 20 °C/min)

sample	MW	mp (°C)	onset (°C)	exomax (°C)	-Δ*H* (cal/mol)
DNAZDN	254	128	147	151	951
DNAZNO$_3$	210	138	148	152	886
DNAZDNT	306	148(dec)	157	161	838
DNAZNTO	277	161(dec)	174	180	435
DNAZCl	183.5	177	188	191	652
TNAZ	192	101	97(endo)	102(endo)	32(endo)
TNAZ			258	278	1085

TGA (Ramp @ 10 (°C/min)

sample	mp (°C)	onset (°C)^a	% wt loss^b	range (°C)^c	% wt^d loss (range)
DNAZDN	128	156	96.8	135−166	87.2
DNAZNO$_3$	138	160	92.4	143−165	74.6
DNAZDNT	148(dec)	170	92.7	144−177	67.1
DNAZNTO	161(dec)	174	94.4	149−206	46.0
				224−292	34.1
DNAZDNI	151(dec)	180	96.2	162−196	28.8
				235−318	42.3
DNAZCl	177	200	97.5	150−212	84.6
TNAZ	101	161	92.2	107−204	91.7

[a] The onset of weight loss. [b] The total weight loss (40−400 °C). [c] The ranges indicate regions of significant weight loss. [d] The weight loss over the specified range.

thermogravimetric analyzer, nitrogen flushing gas, about 0.5 mg size sample, and a scan rate of 10 °C/min from 40−400 °C.

The thermolysis products of TNAZ and dinitroazetidium salts were analyzed by a Varian 3400 gas chromatograph equipped with a capillary column (J&W DB-5MS, 30 m × 0.25 mm i.d.) and interfaced to a Finnigan-MAT TSQ-700 tandem mass spectrometer (injector temperature 200 °C; transfer line 220 °C; injection volume 1 μL). The oven temperature was held at 80 °C for 1 min and then ramped at 7.5 °C/min to 210 °C. Electron impact (EI) and chemical ionization (CI) were at 70 eV with emission currents of 400 μA. The ion source was operated at 150 °C. Methane was used as the CI reagent gas. Collision-induced dissociation experiments were carried out at collision energy 15 eV, with 0.5−1 mTorr (1 Torr = 133.3 Pa) of argon as the collision gas. A solids probe (25−35 °C) was also used to introduce TNAZ into the source of the mass spectrometer. This latter method of introduction yielded mass spectra identical to those obtained using the GC interface.

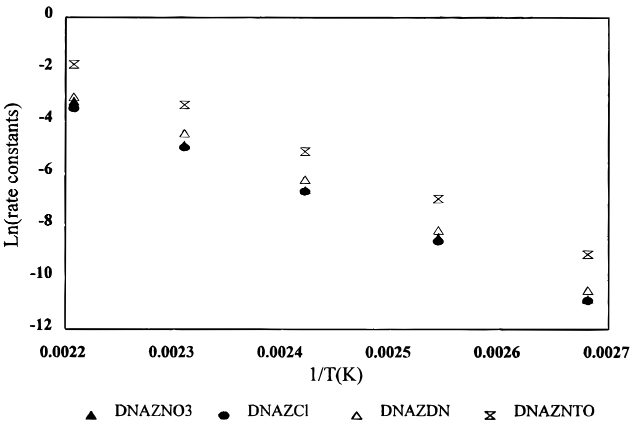

Figure 6. Arrhenius plots of DNAZ$^+$ salts, 1% in water, analyzed for DNAZ$^+$ remaining.

Results

TNAZ Kinetics. Table 1 lists the TNAZ rate constants obtained from first-order plots over the temperature range 160−280 °C. Like the nitramines previously examined,[1,2] neat TNAZ at all temperatures was observed to decompose according to first-order kinetics out to 90% decomposition. The Arrhenius plot of these rate constants is shown in Figure 2 along with plots for other energetic materials showing activation energies (E_a) and pre-exponential factors (A): TNAZ ($E_a = 46.6$ kcal/mol; $A = 3.55 \times 10^{17}$ s^{-1}); HMX ($E_a = 52.9$ kcal/mol; $A = 2.46 \times 10^{18}$ s^{-1}); TNT ($E_a = 41.0$ kcal/mol; $A = 4.44 \times 10^{12}$ s^{-1}); RDX ($E_a = 37.8$ kcal/mol; $A = 1.99 \times 10^{14}$ s^{-1}). Compared to other commonly used explosives (Figure 3), the thermal stability of TNAZ is better than that of RDX but worse than that of HMX or TNT.

In benzene solution TNAZ decompositions were first-order, with rates and activation energies similar to neat TNAZ (Table 1). (For RDX and HMX a similar observation was made; that is, there was little difference between the rate of the neat and the rate of the solution decomposition.) However in methanol and acetone, the TNAZ decomposition rate increased (Figure 4). The increase in TNAZ decomposition rate and variety of decomposition products indicated a TNAZ/methanol reaction.

Decomposition kinetics were examined for the presence of a deuterium kinetic isotope effect (DKIE). A small DKIE (1.31 and 1.38, respectively) was observed when neat TNAZ or TNAZ-d_4 (1% in benzene) was thermolyzed at 240 °C. In the solvents in which TNAZ/solvent interaction (methanol and acetone) occurred, a large DKIE was measured (Table 1); however, no DKIE was observed when TNAZ was heated in deuterated benzene. From these results, we concluded there was no intermolecular DKIE and only a small intramolecular one, a result mirroring our observations with RDX and dimethylnitramine. As is the case with nitramines, nitric acid and diphenylamine (NO$_2$ scavenger) additives affected the TNAZ decomposition rate only slightly (Table 1), whereas TNAZ, like TNT, was reactive with ammonia, immediately forming a brown residue. TNAZ in admixture with RDX exhibited a 2-fold increase in decomposition rate at 200 °C (Table 1).

Dinitroazetidium Salt Kinetics. The decomposition kinetics of dinitroazetidium (DNAZ$^+$) salts (Figure 5) were examined by DSC and by TGA (Table 2). The DSC exothermic maxima for all the dinitroazetidium salts appear at lower temperatures than that for TNAZ. This is in agreement with isothermal studies of these salts which determined decomposition rate constants at 150 °C in the range 10^{-2} s^{-1}, whereas the calculated rate constant for TNAZ at the same temperature is about 10^{-6} s^{-1}. With the exception of TNAZ, relative ordering of thermal stabilities observed by TGA is the same as by DSC: DNAZ

TABLE 3: Rate Constants (s^{-1}) and Kinetics Parameters of DNAZ Salts

Neat

	$DNAZNO_3$					
T (°C)	$DNAZ^+$	NO_3^-	total gas	ASTM[a]	DNAZCl ASTM[a]	DNAZDN total gas
100						4.17E−04
120	3.14E−03[b]	1.08E−03	1.59E−03			1.98E−03
140	2.73E−02	3.02E−03	4.48E−03			5.38E−03
160	9.54E−02	7.50E−03	7.34E−03			9.07E−03
170	2.09E−01	4.59E−02				
180	3.61E−01	8.33E−02				
E_a (kcal/mol)	27.6	16.4	16.8	21.7	49.8	19.1
A (s^{-1})	8.7E+12	1.5E+06	3.6E+06	4.1E+9	1.3E+22	6.9E+07
R^2	0.992	1.00	1.00	0.995	0.972	0.993

1% DNAZ Salts in Aqueous Solutions

	$DNAZNO_3$		DNAZCl	DNAZDN		DNAZNTO
T (°C)	$DNAZ^+$	NO_3^-	$DNAZ^+$	$DNAZ^+$	DN^-	$DNAZ^+$
100	2.00E−05	3.06E−06	1.89E−05	2.80E−05	9.53E−07	1.11E−04
120	2.05E−04	2.16E−05	1.86E−04	2.83E−04	1.22E−05	9.37E−04
140	1.32E−03	9.21E−05	1.26E−03	1.97E−03	1.02E−04	5.79E−03
160	7.50E−03	4.56E−04	6.83E−03	1.17E−02	8.98E−04	3.48E−02
180	3.55E−02	1.54E−04	3.05E−02	4.31E−02	5.83E−03	
200		4.65E−03			3.11E−02	
E_a (kcal/mol)	31.5	25.0	30.9	32.2	36.5	30.6
A (s^{-1})	6.4E+13	1.8E+09	2.8E+13	2.2E+14	2.2E+15	9.7E+13
R^2	0.999	0.999	1.00	0.999	1.00	0.999

[a] ASTM method E698-79. [b] Read as 3.14×10^{-3}.

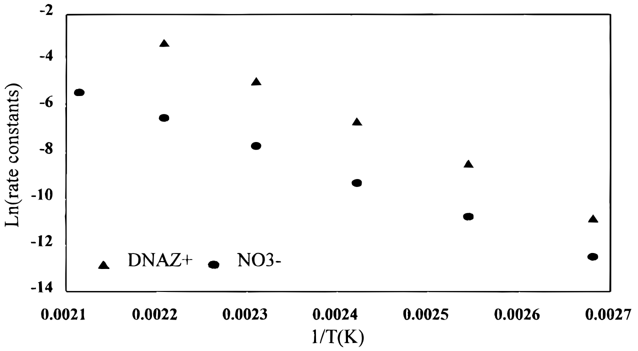

Figure 7. Arrhenius plots of $DNAZ^+NO_3^-$, 1% in water, analyzed for cation and anion remaining.

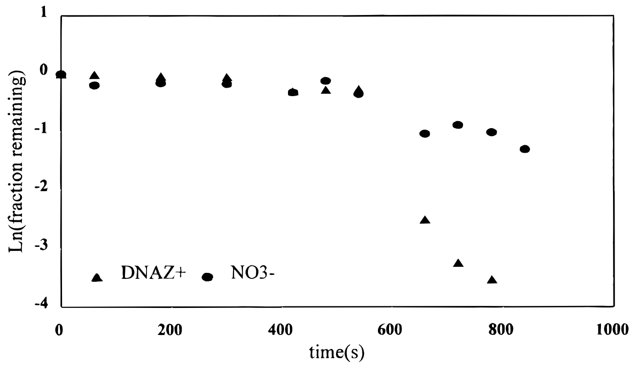

Figure 8. First-order plots of $DNAZ^+NO_3^-$ neat at 120 °C, analyzed for cation and anion remaining.

TABLE 4: Decomposition of Aqueous (1%) $DNAZ^+X^-$ Salts at 140 °C

acid	pK_a	X^-	k (s^{-1}) (for $DNAZ^+$)
HCl	−7.0	Cl^-	1.25E−03[a]
HN_3O_4	−5.62	$N(NO_2)_2^-$	1.97E−03
HNO_3	−1.34	NO_3^-	1.32E−03
NTO	+3.67	NTO^-	5.79E−03

[a] Read as 1.25×10^{-3}.

TABLE 5: Moles of Gas per Mole of DNAZ Salts Heated for 10 Half-Lives

sample	N_2	N_2O	CO_2	CO	NO	total	temp (°C)
Neat (mole gas/mole DNAZ salt)							
DNAZDN	1.06	1.72	1.35	0.10	0.03	4.26	100
DNAZDN	1.12	1.38	1.14	0.25	0.00	3.89	120
DNAZDN	1.15	1.64	1.48	0.25	0.00	4.52	140
DNAZDN	1.33	1.73	1.54	0.33	0.09	5.02	150
DNAZDN	0.72	1.17	1.30	0.49	0.96	4.64	240
$DNAZNO_3$	1.04	0.61	1.31	0.12	0.46	3.54	120
$DNAZNO_3$	1.17	0.51	1.38	0.22	0.10	3.39	140
$DNAZNO_3$	1.18	0.45	1.36	0.35	0.29	3.63	150
$DNAZNO_3$	0.70	0.13	1.2	0.46	0.72	3.21	240
DNAZCl	0.81	0.16	0.63	0.39	0.14	2.13	160
DNAZCl	0.71	0.03	0.44	0.34	0.47	1.99	240
1−2% DNAZ Salts in H_2O at 160 °C							
DNAZDN	1.08	1.25	1.10	0.08	0.0	3.51	
$DNAZNO_3$	0.82	0.64	0.97	0.00	0.0	2.43	
DNAZCl	0.41	0.34	0.33	0.00	0.0	1.08	

DN ~ $DNAZ(NO_3)$ ~ $TNAZ_{TGA}$ < DNAZ DNT < DNAZ NTO < DNAZ Cl < TNAZ $_{DSC}$.

Discrepancy in the TGA we attribute to sublimation of TNAZ, which leads to early weight loss. Some of the 3,3-dinitroazetidium salts ($DNAZ^+$) were examined in more detail: chloride (Cl^-), nitrate (NO_3^-), dinitramidate (DN^-), and the anion of NTO. In aqueous solution (1%) disappearance of the dinitroazetidium cation was first-order, and the rate was very similar for all four dinitroazetidium salts (Figure 6). The cation of the $DNAZ^+$ NTO^- salt decomposed somewhat faster than the other salts. For all four salts in solution as well as neat, the dinitroazetidium cation disappeared faster than the anion, e.g. $DNAZ^+(NO_3^-)$ as shown in Figures 7 and 8. With thermolysis of the neat salts [$DNAZ^+Cl^-$ and $DNAZ^+(NO_3)^-$], the disappearance of the cation was significantly faster than that of the anion (Figure 8). While the decomposition kinetics of the aqueous solutions of the dinitroazetidium salts were first-order, first-order plots of the decomposition of the neat salts were nonlinear after the first 30−40% decomposition (Figure 8). A slight yellowing of the salts indicated the onset of accelerated loss of the cation. Condensed-phase rate constants shown in Tables 3 and 4 are derived from the first 30% decomposition.

Products of Dinitroazetidium Salt. For only three of the dinitroazetidium salts [DNAZCl, $DNAZ(NO_3)$, DNAZDN] did we have sufficient sample to examine the decomposition products. Table 5 shows the gas composition after complete (10 half-lives) decomposition as a function of thermolysis temperature. Only for NO is composition markedly affected by the thermolysis temperature; it increases with temperature.

TABLE 6: Isotopic Distribution of Labeled Isomers for $DNAZNO_3$ (50% dec) and TNAZ at 240 °C (75% dec)

	DNAZ-3-^{13}C-^{15}NO$_3$[a]			DNAZ-^{15}N-^{15}NO$_3$[b]				TNAZ3-^{13}C[c]	TNAZ-^{15}N[d]	TNAZ-N-^{15}N[e]	TNAZ3-^{13}C-N-^{15}N[f]
	100 °C	150 °C	200 °C	100 °C	150 °C	150 °C[g]	200 °C	240 °C[i]	240 °C[i]	240 °C[i]	240 °C[i]
N_2	19.7	36.2	42.9	0.5	0.3	0.3	14.8	99.0	2.8	43.0	40.0
$N^{15}N$	75.7	59.3	53.7	89.0	83.3	76	72.3	1.0	68.9	51.6	53.5
$^{15}N^{15}N$	4.6	4.5	3.4	10.5	16.4	23.7	12.9	0	28.3	5.4	6.5
NO	N.D.[h]	45.5	47.1	N.D.	2.2	0.8	3.0	99.4	4.4	54.1	52.3
^{15}NO	N.D.	54.5	52.9	N.D.	97.8	99.2	97.0	0.6	95.6	45.9	47.7
N_2O	6.2	24.5	32.5	0	0.04	0	0.1	98.9	0	34.8	31.5
$N^{15}NO$	37.4	48.7	47.5	2.5	3.4	2.7	11.0	0.89	18.9	50.9	52.3
$^{15}N^{15}NO$	56.4	26.8	20.0	97.5	96.6	97.3	88.9	0.20	81.1	14.2	16.1
CO_2	56.9	65.2	74.3					62.6	98.9	98.8	61.6
$^{13}CO_2$	43.1	34.8	25.7					37.4	1.1	1.2	38.4
CO	64.8	70.5	73.1					77.0	99.4	99.2	75.0
^{13}CO	35.2	29.5	26.9					23.0	0.6	0.8	25.0
HCN	26.4	31.1	35.0	32.1	29.4	29.2	34.1	55.7	40.7	84.6	51.3
$H^{13}CN$	50.2	48.3	52.3					44.3			48.7
$HC^{15}N$				67.9	70.6	70.8	65.9		59.3	15.4	
$H^{13}C^{15}N$	23.4	20.6	12.7								

[a] ^{13}C on C3, ^{15}N on NO_3^-. [b] ^{15}N on all nitro group and NO_3^-. [c] ^{13}C on C3. [d] ^{15}N on all nitro group. [e] ^{15}N on nitramine nitro group. [f] ^{13}C on C3, ^{15}N on nitramine nitro group. [g] 10 $t_{1/2}$. [h] N.D. = not detected. [i] 75% dec.

TABLE 7: Products of Decomposition of Neat DNAZ Salts[f]

	peak code										
	E 176	**G** 131	**I** 192	**J** 130	**K** 147	**L** 175	**M** 169	**N** 200	**O** 223	**S** 214	**S_1** 214
$DNAZNO_3$[a]	l	t	l	t	t	s	s	t			
$DNAZNO_3$[b]	l	t	s			m	t	t		t	
DNAZCl[c]	m		t			l	m	s	s		m
DNAZCl[d]	l		s			m	m	t	s		m
DNAZDN[e]	l	t	m			m	s				

[a] 240 °C, 5 s. [b] 150 °C, 150 s. [c] 196 °C, 1 min. [d] 200 °C, 1 min. [e] 150 °C, 1 min. l = large; m = medium; s = small; t = tiny. [g] Molecular weight.

TABLE 8: Decomposition Products of 1% DNAZ Salts in Solution[a]

		$DNAZNO_3$				
peak code	MW	MeOH[b] 240 °C/ 5 s	MeOH[b] 150 °C/ 300 s	EtOH[b] 150 °C/ 300 s	DNAZCl MeOH[b] 150 °C/300 s	DNAZDN MeOH[b] 150 °C/300 s
A	150	t	s	m	m	m
B	149	t	t			s
C	161		s	t		s
D_2	147	s	s		s	m
E	176	m	l	l	m	l
F	191	s			s	
G	131	m	s	l	t	l
H	191	l			s	
I	192	m	s	s	l	s
J	130	s		t	t	
K	147	s		t	t	t
L	175	s	m	s	s	s
M	169	s	t	s	s	t
N	200	t		t	t	
O	223				s	
S	214	s			t	
S_1	213				t	
T	264	m	t		t	
U	309	l	l	s	l	s
V	322			m		

[a] l = large; m = medium; s = small; t = tiny. [b] Solvent.

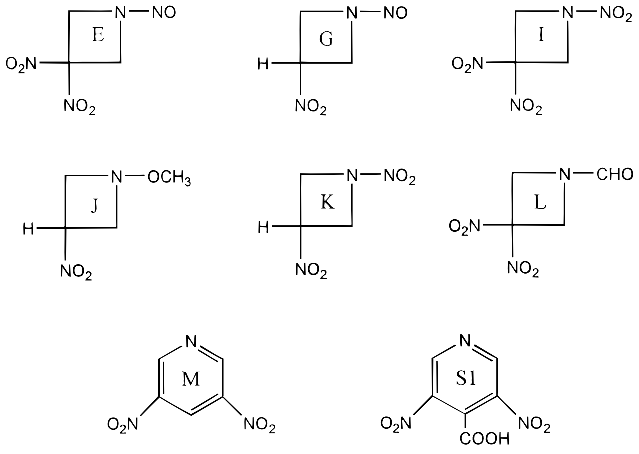

Figure 9. Condense-phase products of neat TNAZ and $DNAZ^+$ salts.

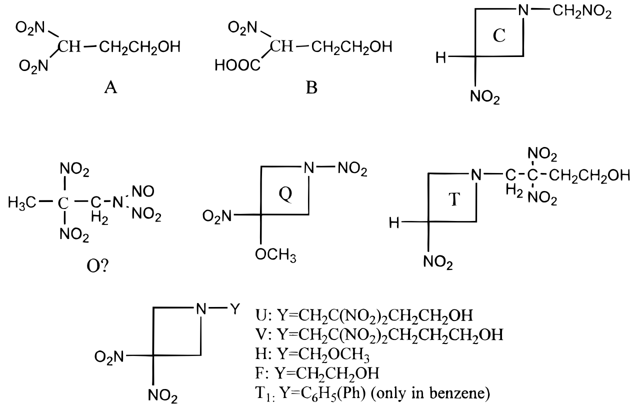

Figure 10. TNAZ and DNAZ products in methanol.

Our analytical techniques did not allow us to quantify NO_2, which was observed when hot samples were first removed from the thermolysis baths. $DNAZ^+Cl^-$ formed the least gas, about 2 mol gas/mol $DNAZ^+Cl^-$; $DNAZ^+(NO_3)^-$ formed about 3.5 mol gas/mol $DNAZ^+(NO_3)^-$; and $DNAZ^+DN^-$ formed the most gas, about 5 mol gas/mol $DNAZ^+DN^-$. Less gas was formed in the aqueous decompositions of the salts than was formed in the neat decompositions: about 1 mol less gas per mol dinitroazetidium salt. Since the anions of both $DNAZ^+DN^-$ and $DNAZ^+(NO_3)^-$ can produce gas, we examined the behavior of $DNAZ^+Cl^-$ to judge the products formed by dinitroazetidium. Formation of 1 mol of nitrogen gas per 1 mol of dinitroazetidium salt is a common feature of the neat decompositions, as is the appearance of 1 mol of carbonaceous gas (0.6 CO_2 and 0.4 CO). Nitrous oxide was only an important gaseous product in the decomposition of the dinitramidate salt, and we have already shown that dinitramidate decomposes producing 1 mol of N_2O and 1 mol of NO_3^-.[11] Small amounts of hydrogen cyanide and cyanogen were also observed. Information as to the origins of these gases can be derived from Table 6, which shows the isotopic distribution of gases derived from $DNAZ^+(NO_3)^-$ labeled with ^{13}C on C3 and ^{15}N on the nitrate ion (DNAZ-3-

TABLE 9: Decomposition Gases of Neat Energetic Materials after Heating 10 Half-Lives

	CO_2%	CO%	N_2O%	N_2%	NO%	total (mol)	temp (°C)
DMN	0.53	0.14	0.02	0.31		0.5	240
DIPN	0.09	0.04	0.09	0.78		0.5	240
RDX	0.20	0.20	0.29	0.31		4.4	240
HMX	0.22	0.11	0.52	0.15		5.4	240
DNAZCl	0.22	0.17	0.02	0.36	0.23	2.0	240
DNAZDN	0.28	0.11	0.25	0.16	0.21	4.6	240
$DNAZNO_3$	0.38	0.14	0.04	0.22	0.22	3.2	240
TNAZ	0.38	0.16	0.03	0.21	0.22	4.0	240
ADN			0.53	0.47		1.9	200
KDN			0.86	0.14		0.6	200

TABLE 10: Distribution of Isotopic Labeled TNAZ in Decomposition Gases

	MW	22 s (10%)	60 s (25%)	143 s (50%)	300 s (75%)	30 m (100%)
Neat TNAZ-N-^{15}N (^{15}N on Nitramine Nitro Group, 240 °C)						
N_2	28	28.4	37.1	38.1	43.0	53.2
$N^{15}N$	29	65.0	57.1	55.7	51.6	42.7
$^{15}N^{15}N$	30	6.5	5.8	6.2	5.4	4.1
NO	30	34.1	37.4	45.9	54.1	71.4
^{15}NO	31	65.9	62.6	54.1	45.9	28.6
N_2O	44	27.7	27.0	28.9	34.8	45.3
$N^{15}NO$	45	56.1	56.9	53.2	50.9	45.2
$^{15}N^{15}NO$	46	16.2	16.1	17.9	14.2	9.4
HCN	27	90.7	90.7	87.7	84.6	83.2
$HC^{15}N$	28	9.3	9.3	12.3	15.4	16.8
Neat TNAZ-3-^{13}C (^{13}C on C3, 240 °C)						
CO	28	58.5	70.5	78.9	77.0	80.0
^{13}CO	29	41.5	29.5	21.1	23.0	20.0
CO_2	44	53.0	57.8	64.3	62.6	63.5
$^{13}CO_2$	45	47.0	42.2	35.7	37.4	36.5
HCN	27	77.9	66.0	53.1	55.7	44.7
$H^{13}CN$	28	22.1	34.0	46.9	44.3	55.3

TABLE 11: GC/MS of Neat TNAZ at 240 °C 5 min, Using CI[c]

	peak codes								
sample	D_1 112[d]	E 176	G 131	I 192	J 130	K 147	L 175	M 169	N 189
TNAZ 10 s		s		l	t	s	s	t	
TNAZ 60 s		s	t	l	t	s	t	t	
TNAZ[a]		l	s	l	t			s	s
TNAZ	t	l	s	l	t	m	m	t	s
TNAZ	t	l	s	l	t	m	m	t	s
TNAZ[a,b]		l	s	l		s	m		t
TNAZN-^{15}N	t	l	s	l	t	m	m	t	m
TNAZ-^{15}N	t	l	s	l	t	m	m	t	m
TNAZ-3-^{13}C	t	l	s	l	t	m	l	t	s
TNAZ-3^{13}C-N-^{15}N		l	s	l	t	m	m	t	s
TNAZ-d_4[a]		l	t	l	s		t	t	

[a] Using electron impact detection. [b] Under the vacuum. [c] l = large; m = medium; s = small; t = tiny. [d] Molecular weight.

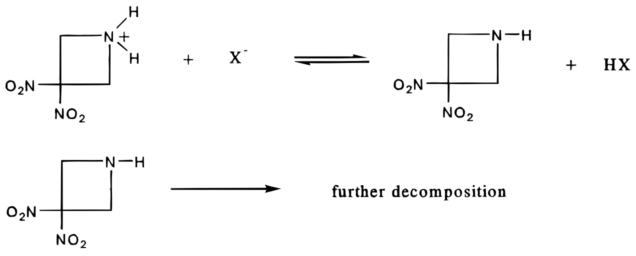

Figure 11. $DNAZ^+$ salts, possible decomposition mechanism.

^{13}C-$^{15}NO_3$) and labeled with^{15}N on both nitro groups and the nitrate ion (DNAZ-^{15}N-$^{15}NO_3$).

In solution all the dinitroazetidium salts formed ammonium and nitrite ions. The dinitramidate salt also formed nitrate. No attempt was made to quantify these ionic products. The decompositions of the neat dinitroazetidium salts were primarily examined for organic products. These products are tabulated in Tables 7 (for neat thermolyses) and 8 (for solution thermolyses) and pictured in Figures 9 and 10. Some of the products (**E**, **K**, **L**, and **M**) were identified using authentic samples. Some are assigned by observing fragmentation patterns and comparing them to that of isotopically labeled $DNAZ^+(NO_3)^-$. Due to insufficient quantities of these decomposition products, no quantitation is possible. Relative amounts can be inferred from the size of the chromatographic peak, as indicated in the tables (l = large; m = medium; s = small, t = tiny). In the case of neat $DNAZ^+(NO_3)^-$, we examined the residue for water-soluble salts and found almost no ammonium ion, in contrast to observations in the aqueous decompositions. We assumed that the counterbalancing cation for the slowly disappearing anion (e.g. Figure 8) is a proton.

Products of TNAZ. The gaseous products of the condensed-phase thermolysis of TNAZ were similar to those of $DNAZ^+(NO_3)^-$ and $DNAZ^+Cl^-$ and to simple nitramines such as dimethylnitramine (DMN) in that the amount of nitrogen produced was much greater than the amount of nitrous oxide (Table 9). Both TNAZ and related dinitroazetidium salts produced more carbon dioxide than any of the pure nitramines examined, and unlike the pure nitramines, they all formed detectable amounts of NO.[1,7,8] Nitrogen was the first nitrogen-containing gas formed. After 20 s heating at 240 °C (roughly 9% decomposition) the gases observed were 0.13 L of N_2, 0.51 L of CO_2, and 0.22 L of CO at STP per mol of TNAZ; no N_2O nor NO was detected. Isotopic distributions of the decomposition gases were determined using TNAZ ^{15}N-labeled only at the nitro group attached to the azetidine nitrogen (TNAZ-N-^{15}N), TNAZ ^{15}N-labeled at all three nitro groups (TNAZ-^{15}N), TNAZ with ^{13}C on C3 (TNAZ-3-^{13}C), and TNAZ with both ^{13}C on C3 and ^{15}N on the nitro group of the azetidine nitrogen (TNAZ-3-^{13}C-N-^{15}N) (Table VI). Table 10 shows the fraction of each isotopically labeled gas as a function of the fraction TNAZ reacted at 240 °C. As in the case of the dinitroazetidium salts, NO_2 was sometimes observed but not quantified.

The NMR spectrum of the TNAZ in acetone solution, previously sealed and heated at 240 °C for 4 min (about 70% conversion), showed only one decomposition product, identified as 1-nitroso-3,3-dinitroazetidine (NO-DNAZ). This identification was confirmed by comparison with an authentic sample [TNAZ ^1H 5.47 ppm; ^{13}C 105 and 65 ppm; ^{15}N 212 N ring; 362 N-NO_2; 366 C−NO_2; NO-DNAZ ^1H 6.03 and 5.17 ppm; ^{13}C 108, 68, and 63 ppm]. In the thermolysis of neat TNAZ, no insoluble residue was observed in partially decomposed samples; but at long decomposition times, neat TNAZ formed a black tarlike residue. A detailed study of the decomposition products was conducted using a tandem mass spectrometer. The results, using GC/MS, are summarized for neat TNAZ and various TNAZ solutions in Tables 11 and 12, respectively. The assignments of molecular weights are based on the CI mass spectrum of each decomposition product. Some of the products (**E**, **K**, **L**, and **M**) were identified using authentic samples. Others are assigned on the basis of their fragmentation patterns and comparison to that of isotopically labeled TNAZ.[12] Relative amounts can be inferred from the size of the chromatographic peak as indicated in the tables (l = large; m = medium; s = small, t = tiny).

Discussion

Decomposition Rates. TNAZ, neat and in benzene, decomposed by first-order kinetics at all temperatures examined, leaving some insoluble residue. In protonic solvents such as water, acetone, or methanol, TNAZ decomposition rate was

TABLE 12: GC/MS of 1% TNAZ in Different Solvents at 240 °C Using CI[a]

		peak codes															
sample	dec (%)	B	D_2	E	F	G	H	I	J	K	M	N	P	Q	S	T_1	U
TNAZ/MeOH 10 s	19			s		t	m	l		m							
TNAZ/CD_3OD 10 s	10			t			s	l		m							
TNAZ/MeOH 40 s	56		t	s	t	s	m	l		l				s			
TNAZ/MeOH 80 s	81	t	t	s	t	m	s	m		l	t		t	m	t		t
TNAZ/MeOH 163 s	96	t	s	s	t	m	t	s		l	t	s	s	m			
TNAZ/MeOH 5 min	99.8	t	s	t		l		s	t	l		s	s	m	t		
TNAZ/MeOH 13 min	100	s		t		l		s		m			t				
TNAZ/H_2O 46 s	50			t		t		l		m							
TNAZ/acetone 163 s	75			m		t		l		s							
TNAZ/acetone 5 min	92			l		s		m		s							
TNAZ/C_6D_6 10 s	5			t				l		t							
TNAZ/C_6H_6 3 min	62			l				l		t		t				s	
TNAZ/C_6D_6 3 min	60			l		t		l		s	t					s	

[a] l = large; m = medium; s = small; t = tiny.

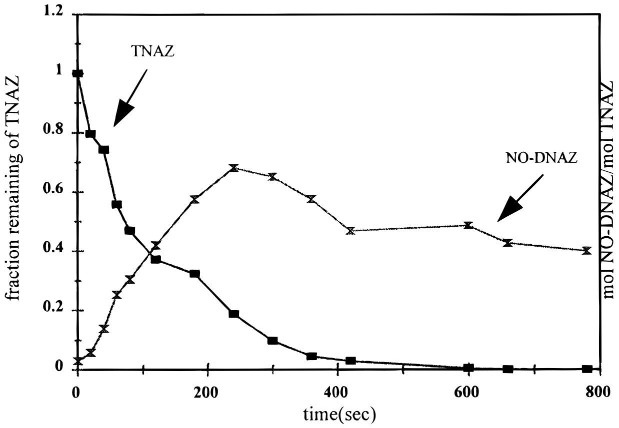

Figure 12. Thermolysis of TNAZ in acetone (1%) at 240 °C. The decomposition of TNAZ (fraction remaining) and the formation of NO-DNAZ (mol NO-DNAZ/mol TNAZ) are included.

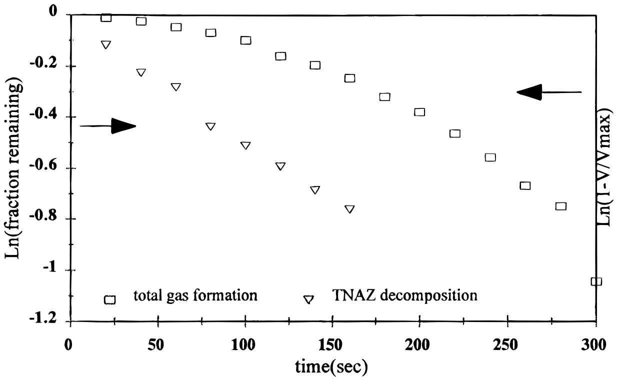

Figure 13. First-order plot of neat TNAZ thermolysis at 240 °C, monitoring TNAZ loss and gas formation.

enhanced 2- to 4-fold, and a DKIE was exhibited in deuterated solvent (Table 1). These observations and the fact that the activation energy of decomposition is about 10 kcal/mol lower in methanol than in benzene (Table 1) suggest homolysis decomposition pathways, dominant in aprotic solvents, are overwhelmed by a hydrogen transfer pathway in protonic solvents. In nitroarenes competition between $C-NO_2$ homolysis and a pathway where hydrogen transfer to the nitro group assists $C-NO_2$ bond breakage is well-known.[13]

Neat dinitroazetidium salts decompose in a first-order fashion to about 30−40% decomposition and then show accelerated decomposition, which leaves no insoluble residue. The dinitroazetidium salts have markedly less thermal stability than TNAZ; their order of thermal stability in water roughly follows the acidity of the parent acid (Table 4). These results suggest a mechanism that involves proton transfer from the dinitroazetidium cation to form DNAZ. DNAZ, regardless of its salt of origin, decomposes at approximately the same rate (Figure 11). The autocatalytic nature of the reaction may be a result of the basic nature of the decomposition products of DNAZ.

Gaseous Products. The TNAZ and the dinitroazetidium salts formed similar distributions of gaseous decomposition products: 2−3 times as much CO_2 as CO, about equal ratios of NO to N_2 (at 240 °C), and with the exception of $DNAZ^+DN^-$, significantly more N_2 than N_2O (Tables 5 and 9). Experiments with isotopically labeled $DNAZ^+(NO_3)^-$ indicated that most of the nitrogen gas contained one azetidium nitrogen, while NO and N_2O were formed almost exclusively from the nitrate and nitro groups (50% decomposition, 150 °C, Table 6). The CO and CO_2 are formed more or less equally from all three carbons. At 100 °C, nitrogen-containing gases and CO_2 contain more nitrate nitrogen and C3, respectively.

Analysis of the decomposition gases from the labeled TNAZ shows the fate of the nitro group attached to the azetidine nitrogen; it is responsible for a disproportionate share of the early formation of NO, N_2O, and N_2 (Table 10). In the early stages of the reaction (10% decomposition) 66% of the NO comes from the nitro group on the azetidine, but by completion of the reaction all three nitro groups contribute equally to the NO composition. The azetidine nitrogen, at most, accounts for 4% of the total NO (Table 6). The fact that at early decomposition the contribution from the nitro group on the azetidine is disproportionately high suggests at 240 °C the $N-NO_2$ bond is preferentially broken over the $C-NO_2$ bond. Analysis of the fate of the labeled C3 shows that the label is disproportionately high in the carbonaceous gases at early stages of decomposition, but decreases to roughly a third of the CO_2 and less than a fifth of the CO, suggesting this is the first carbon oxidized (Table 6).

Condensed-Phase Products. Mass spectra indicate that 1-nitroso-3,3-dinitroazetidine (NO-DNAZ, **E**) is the major decomposition product of neat TNAZ and TNAZ in benzene or acetone solutions (Tables 11 and 12). It is also the major decomposition product of $DNAZ^+Cl^-$, $DNAZ^+(NO_3)^-$, and $DNAZ^+DN^-$, neat or in methanol (Tables 7 and 8). These three dinitroazetidium salts share a number of decomposition products in common with TNAZ: **I**, **E**, **L**, **M**, **G**, **J**, **K**, **N**, **O** (in order of abundance) (Figure 9). This is not surprising since TNAZ (**I**) is a product of their decompositions (Table 7). When the dinitroazetidium salts or TNAZ is heated in methanol or ethanol solution, they form decomposition products that show solvent attachment to the nitrogen of the azetidium ring as well as products resulting from ring cleavage (Tables 8 and 12, Figure 10). Even in benzene a product T_1 was identified were the phenyl ring is attached to the azetidium nitrogen. Assignments for the attachment to the azetidine nitrogen rather than to C3

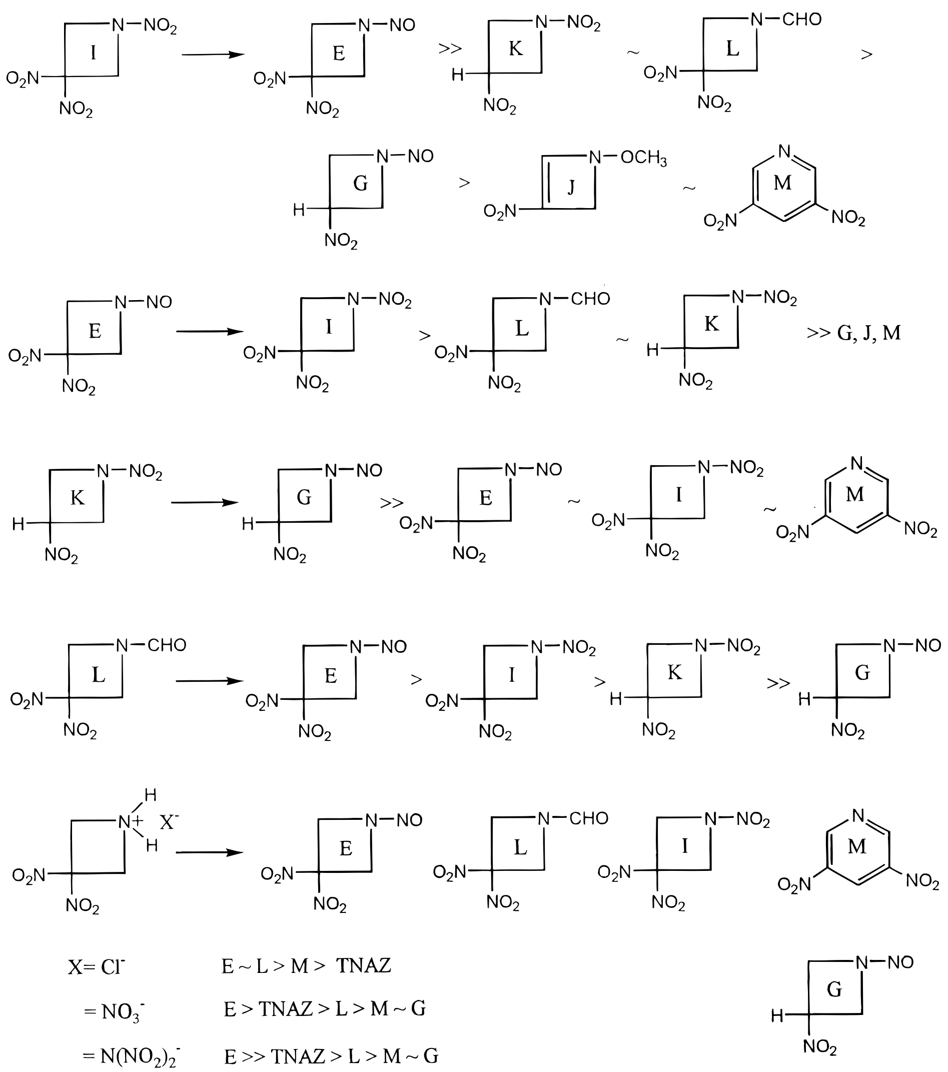

Figure 14. Principal decomposition products of TNAZ and its decomposition products (MS/MS study).

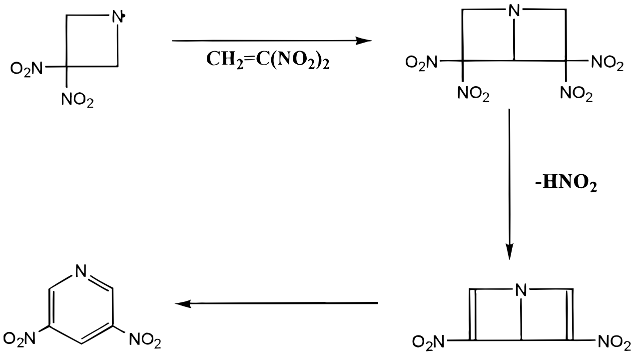

Figure 15. Proposed formation of 3,5-dinitropyridine.

are based on labeling studies, especially noting the loss of ^{15}N from TNAZ- N-^{15}N. This may be interpreted as indicative that N$-$NO$_2$ scission is more predominant than C$-$NO$_2$, although other interpretations are possible. For example, K is the major decomposition product when TNAZ is heated in methanol, ethanol, or water (Table 12). This indicates C$-$NO$_2$ scission does occur, but perhaps, unlike the amine radical, the C3 radical can only be easily capped by H$^\bullet$ rather than by a larger hydrocarbon originating from the solvent.

SCHEME 1: TNAZ Decomposition Mechanism

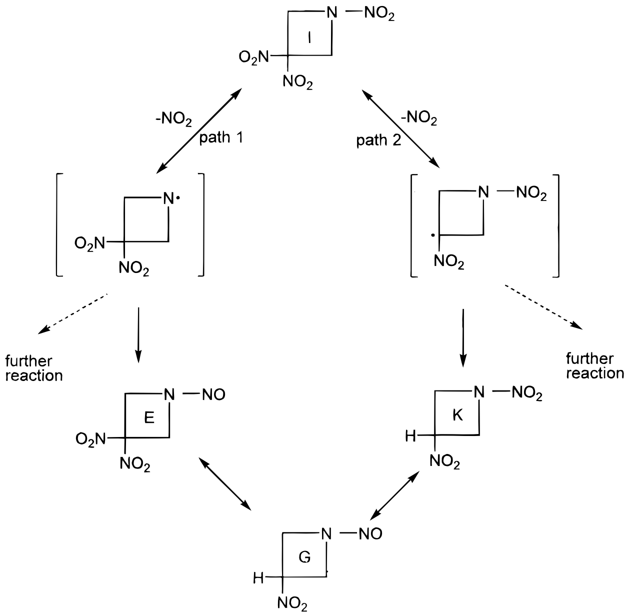

The species observed from TNAZ decomposition are the same as observed in the decomposition of the dinitroazetidium salts (Table 11, neat TNAZ, and Table 12, TNAZ solutions). The compounds coded as **E**, **K**, **L**, and **M** were identified by comparison with authentic samples. While NO-DNAZ (**E**) is the first and most abundant product observed under the conditions of these experiments, next in terms of amount and order of formation are 1,3-dinitroazetidine (**K**) and 1-formyl-3,3-dinitroazetidine (**L**), respectively. We speculate that 1$-$nitroso-3,3-dinitroazetidine (NO-DNAZ, **E**) is the first TNAZ

SCHEME 2: General Reaction Scheme for TNAZ and DNAZ Salts

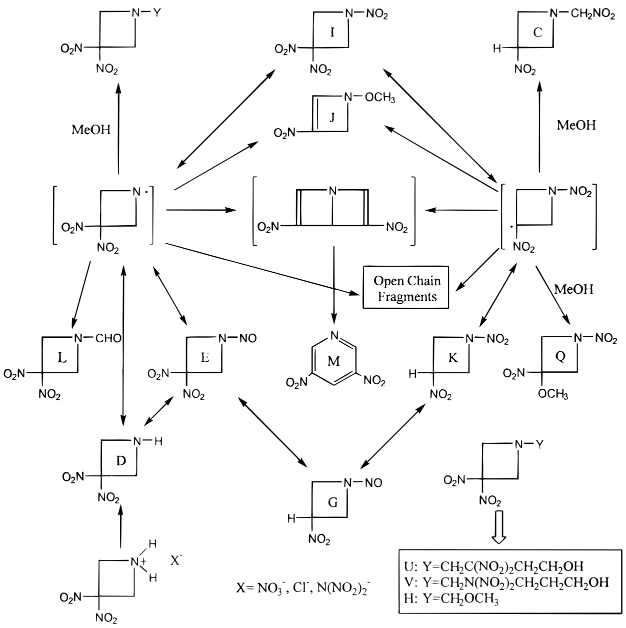

TABLE 13: GC/MS of Neat NO-DNAZ, K[a], and L[b] at 240 °C Using CI[c]

sample	**D**$_1$ 112[d]	**E** 176	**G** 131	**I** 192	**J** 130	**K** 147	**L** 175	**M** 169	**N** 189
NO-DNAZ(**E**)/1 min	t	m	s	l	t	s	m	t	s
NO-DNAZ(**E**)/5 min		l	s	m	t	s	m	s	t
K/5 min			t	t		l			
K/10 min		s	m	s		l		s	
L/5 min		l	s	m		m	l		

[a] 1,3-Dinitroazetidine (**K**). [b] 1-Formyl-3,3-dinitroazetidine (**L**). [c] l = large; m = medium; s = small; t = tiny. [d] Molecular weight.

product formed. However, under the conditions of these experiments, it decomposes at an appreciable rate. Figure 12 shows the rate of TNAZ disappearance (1% in acetone) along with the rate of NO-DNAZ (**E**) appearance. The concentration of the latter quickly reaches a plateau. In the decomposition of neat TNAZ, gas formation was slower than TNAZ loss, we believe this is due to the fact that TNAZ forms condensed-phase products that decompose at different rates to ultimately form the gases (Figure 13). In contrast to NO-DNAZ (**E**), 1,3-dinitroazetidine (**K**) is quite stable. A comparison of the DSC (20 °C/min) shows that TNAZ and **K** (exothermic maxima 275 and 274 °C, respectively) are significantly more stable than **L** and NO-DNAZ (exothermic maxima 247 and 246 °C, respectively). The thermal stability of NO-DNAZ relative to TNAZ is reversed in acetone. While neat NO-DNAZ is definitely less stable than TNAZ, in acetone NO-DNAZ decomposes more slowly than TNAZ (TNAZ $k = 8.47 \times 10^{-3}$ s^{-1} and NO-DNAZ $k = 1.57 \times 10^{-3}$ s^{-1} at 240 °C). The acetone stabilization of the nitroso decomposition products of nitramines has previously been observed for RDX.[2]

A tabulation of the decomposition products of **E**, **K**, and **L** is given in Table 13 and schematically illustrated in Figure 14. The reaction scheme of TNAZ is complex because **I**, **E**, **K**, and probably **G** can interconvert with each other (Scheme 1). Although 1-formyl-3,3-dinitroazetidine (**L**) can form **I** and **E** and vice versa, **L** differs from the other azetidine products in that its formation must sacrifice another azetidine to provide a carbon source. 3,5-Dinitropyridine (**M**) is a minor product of all the dinitroazetidine decompositions; it is formed by thermal ring cleavage and subsequent cycloreversion (Figure 15). An intertwining scheme of products is shown in Scheme 2. Products **E** and **K** are the first and second products in terms of which products are formed first and in terms of which products are formed in greatest abundance. Product **K** is the more stable of the two. Products **E** and **K** are linked through 1-nitroso-3-nitroazetidine (**G**). An authentic sample of **K** was observed to form both **G**, **E**, and TNAZ, while **E** has been observed to form **G**, **K**, **L** and TNAZ.

Conclusions

These results are consistent with two important decomposition pathways for TNAZ: one via $N-NO_2$ bond homolysis and one via $C-NO_2$ cleavage. Under the conditions of these experiments, $N-NO_2$ is favored, although its dominance is not huge; 66% of the initial (10% decomposition) NO formed was observed (by ^{15}N-labeling experiments) to come from the nitro group on the azetidine nitrogen. The activation energy for TNAZ decomposition (46.6 kcal/mol) is similar to that of pure nitramines.[2] A small DKIE (1.4) was observed as well as a sensitivity to ammonia; these may result from the $C-NO_2$ cleavage pathway in which hydrogen transfer to the nitro group may assist in bond breakage. This conclusion is consistent with the observed enhanced decomposition of TNAZ in protonic solvents.

Acknowledgment. We thank Dr. Richard Miller of the Office of Naval Research for funding this work.

References and Notes

(1) Oxley, J. C.; Hiskey, M. A.; Naud, D.; Szekeres, R. *J. Phys. Chem.* **1992**, *96*, 2505−2509.

(2) Oxley, J. C.; Kooh, A. B.; Szekeres, Zheng, W. *J. Phys. Chem.* **1994**, *98*, 7004−7008.

(3) Archibald, T. G.; Gilardi, R.; Baum, K.; George, C. *J. Org. Chem.* **1990**, *55*, 2920−2924.

(4) Lyer, S.; Eng, Y. S.; Joyce, M.; Perez, R.; Alster, J.; Stec, D. *Proceedings of ADPA Manufacture Compatibility of Plastics and other Materials with Explosives, Propellants, Pyrotechnics and Processing of Explosives, Propellants, and Ingredients*, San Diego, CA, April 1991, p 80.

(5) Politzer, P.; Seminario, J. M. *Chem. Phys. Lett.* **1993**, *207*, 27−30. Murray, J. S.; Seminario J. M.; Lane, P.; Politzer P. *J. Mol. Struct. (THEOCHEM)* **1990**, *207*, 193−200.

(6) Mc Kenney, R. L.; Marchand, A. Submitted *J. Energ. Mater.*

(7) Anex, D. S.; Allman, J. C.; Lee, Y. T. In *Chemistry of Energetic Materials*; Olah, G. A., Squire, D. R., Eds.; Academic Press: New York, 1991; Chapter 2.

(8) Oyumi, Y.; Brill, T. B. *Combust. Flame* **1985**, *62*, 225−231.

(9) Coburn, M. D.; Hiskey, M. A.; Oxley, J. C.; Smith, J. L.; Zheng, W.; Rogers, E. *J. Energ. Mater.* submitted.

(10) Zheng, W.; Dong, X. X.; Rogers, E.; Oxley, J. C.; Smith, J. L. *J. Chromat. Sci.*, submitted.

(11) Oxley, J. C.; Smith, J. L.; Zheng, W.; Rogers, E.; Coburn, M. D. *J. Phys. Chem.*, submitted.

(12) Zheng, W.; Rogers, E.; Coburn, M. D.; Oxley, J. C.; Smith, J. L. *J. Mass Spectrom.* submitted.

(13) Minier, L.; Brower, K.; Oxley, J. C. *J. Org. Chem.* **1991**, *56*, 3306−3314.